ISSN: 2710-0723

Effects of Two- and Three-Dimensional Morphological and Structural Greening Characteristics of Street Trees on the Street Thermal Environment

Wei Yang, Mingjie Zhang, Zichen Zhao, Wenting Wang, and Hai Yan*

Zhejiang A&F University, Hangzhou, China

*Corresponding Author

Abstract

Under extreme heat conditions, street trees play a vital role in mitigating the urban street thermal environment. However, the relative contributions of their two- and three-dimensional greening structural characteristics remain insufficiently quantified. This study examined the differential effects of two- and three-dimensional greening indices on street thermal conditions. Mobile measurements were conducted on typical streets in Hangzhou during the summer of 2024 to collect daytime and nighttime meteorological data. Fisheye images and semantic segmentation were used to extract greening structural indicators, which were classified into two- and three-dimensional metrics based on previous studies. The results showed that, compared with treeless streets, streets with high canopy cover reduced daytime air temperature by 2.76°C ($p < 0.01$). Three-dimensional indicators showed significant daytime cooling effects, with GVI, TVF, and CV most strongly associated with air temperature (Ta), whereas the two-dimensional indicator TCR showed a slight nighttime warming effect. The effects of street-tree greening structure on air temperature were spatially scale-dependent, with an optimal range of about 70–110 m; the best-fit interval was 100–110 m during the day and around 100 m at night. These findings provide empirical support for street-greening optimization and climate-adaptive urban design.

Keywords

Street Thermal Environment; Street Trees; Three-Dimensional Greening Structural and Morphological Indices; Air Temperature; Scale Effect.

1. Introduction

Global warming and rapid urbanization have intensified the Urban Heat Island (UHI) effect, making it a major environmental challenge for cities worldwide [1], [2]. UHI not only increases urban energy consumption and greenhouse gas emissions, but also reduces outdoor thermal comfort and raises the risks of heat-related illness and mortality [3], [4]. Under increasingly frequent extreme heat events and heatwaves, street canyons are particularly vulnerable to thermal stress due to extensive impervious surfaces, restricted ventilation, and heat accumulation [2], [5].

Previous studies have shown that street thermal environments are jointly shaped by street geometry and vegetation configuration. Geometric factors such as street orientation, aspect ratio (AR), building height (BH), and sky view factor (SVF) affect radiative exchange, heat storage, and air circulation within street canyons [6]–[8]. Street trees, as the dominant form of street greenery, mitigate heat exposure through canopy shading and transpiration-driven latent heat exchange [9]–[11]. Many studies have confirmed their cooling effects on near-ground air temperature and pedestrian-level thermal stress [12]–[14]. However, these effects depend not only on tree species, but also on greening morphological and structural

ISSN: 2710-0723

characteristics. Variations in diameter at breast height (DBH), tree height (TH), crown width (CW), and trunk branch height (TBH) can lead to substantial differences in shading capacity, transpiration potential, and canopy organization, thereby producing heterogeneous cooling effects [15]–[18].

Although the thermal regulation function of street trees has received increasing attention, most studies still rely on single indicators to describe vegetation structure and have not fully clarified the distinct roles of different street-tree greening characteristics in shaping street thermal conditions. Existing research has mainly focused on two-dimensional or individual-tree metrics, such as tree canopy coverage (TCR), DBH, TH, and CW, while paying less attention to three-dimensional indicators that better reflect canopy spatial structure and pedestrian-level visual perception [19]–[22]. In contrast, green view index (GVI), tree view factor (TVF), crown volume (CV), and canopy thickness (CT) can better characterize the spatial occupation of tree canopies and are more directly related to shading intensity, radiative exchange, and heat transfer in street canyons [23]–[25].

Moreover, the thermal effects of street-tree structure show clear diurnal variation. During the daytime, canopy shading and transpiration usually dominate the cooling process; at night, denser canopy cover and stronger spatial enclosure may suppress longwave heat release and near-surface air exchange, thereby reducing nocturnal cooling efficiency [16], [26], [27]. In addition, the relationship between street-tree structure and thermal environment is scale-dependent. Small analysis extents may fail to capture overall greening patterns, whereas excessively large buffers may obscure local microclimatic characteristics [28]–[30]. Therefore, both diurnal variation and spatial scale should be considered when examining the thermal regulation effects of street trees.

Methodological limitations also remain. Satellite remote sensing and fixed-site observations are often constrained by spatial resolution and temporal continuity, making it difficult to capture fine-scale thermal variations at the street level [31]–[33]. Meanwhile, many studies are based on relatively small street-tree samples, limiting a comprehensive understanding of the relationship between street-tree structure and street air temperature. Studies combining high-resolution mobile measurements of daytime and nighttime air temperature with quantitative assessments of both two- and three-dimensional street-tree structural characteristics across multiple spatial scales remain scarce.

To address these gaps, this study focuses on street spaces in Lin'an District, Hangzhou, and investigates the effects of street-tree greening morphological and structural characteristics on street air temperature using mobile measurements and high-resolution greening structure extraction. Specifically, this study aims to: (1) identify differences in thermal regulation among different street-tree greening characteristics; (2) compare the relative contributions of two- and three-dimensional structural indicators to street air temperature and clarify their mechanisms; and (3) determine the key factors affecting the street thermal environment and explain how they influence cooling performance.

2. Methods

2.1. Study Area Overview

The study area is located in Hangzhou, China (119°00′–119°12′ E, 30°11′–30°16′ N), with relatively flat terrain and an elevation of 45–50 m. It has a subtropical monsoon climate (Cfa, Köppen–Geiger classification), with an annual mean temperature of 16.9 °C, annual precipitation of 1628.6 mm, average relative humidity of 79.0%, and annual sunshine duration of 1847.3 h (China Meteorological Administration, 2024). The total length of the surveyed roads was approximately 19.8 km, with an average width of 23.36 m. The streets varied markedly in

ISSN: 2710-0723

typology and street-tree morphology, making the area suitable for comparative research on street thermal environments under different structural characteristics.

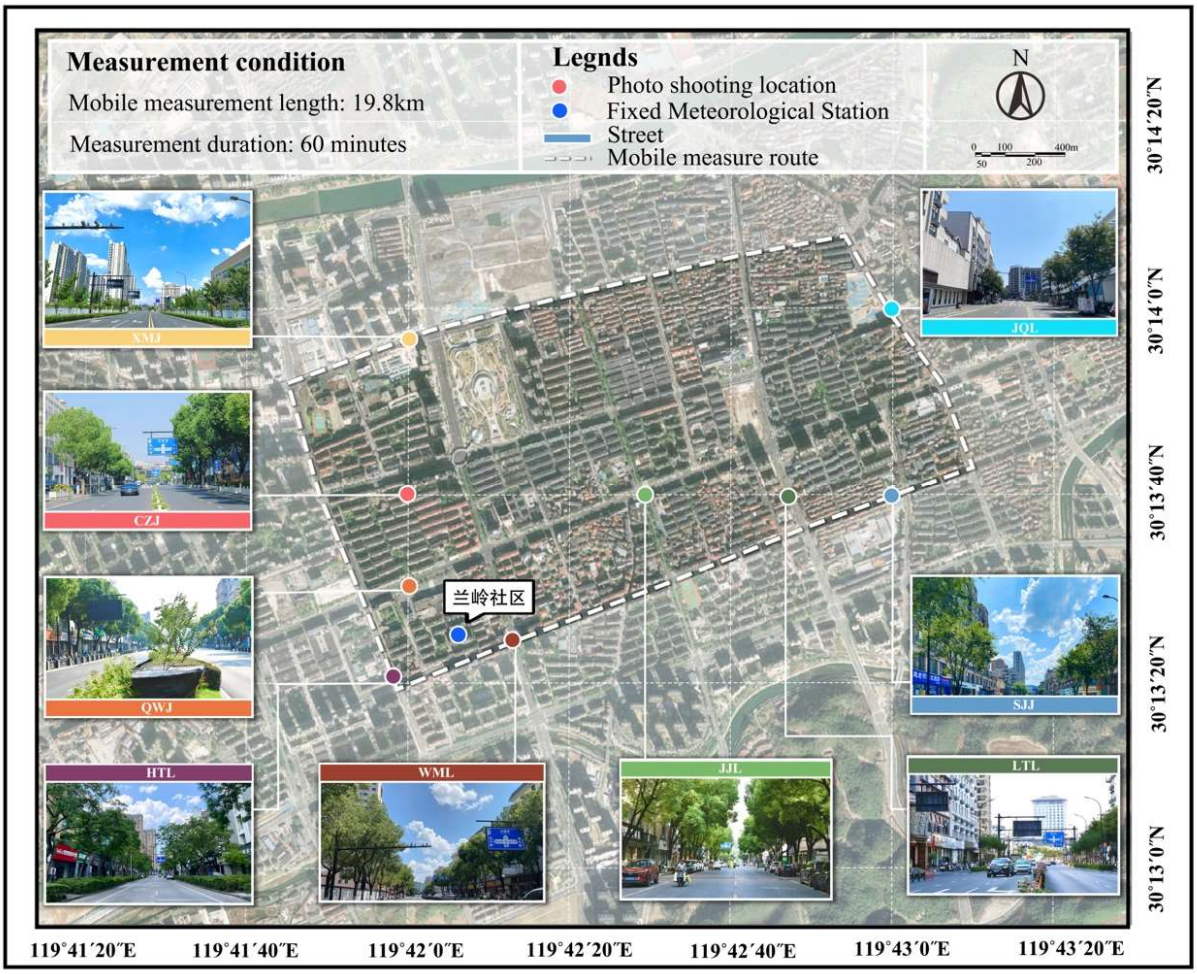

Figure 1. Site information and street characteristics.

2.2. Urban Street Microclimate Measurement

This study employed a mobile measurement approach to efficiently obtain high-spatial-resolution microclimate data at the street scale along predetermined routes. The field experiment was conducted continuously for seven days, from 5 August to 10 August 2024, under weather conditions with low cloud cover and low wind speed, so as to minimize interference from external environmental variables during mobile data collection. Two measurement periods were selected: 14:00–15:00, representing the daytime peak air temperature period [34], and 22:00–23:00, corresponding to the period when the urban heat island effect is strongest. These time periods also avoided traffic peak hours, thereby reducing thermal disturbance caused by vehicles and pedestrian activities. Meanwhile, background meteorological data were obtained from the Donghu Village and Lanling Community weather stations in Lin'an District, Hangzhou, including air temperature, relative humidity, wind speed, and wind direction (WD). To reduce the influence of daily anomalies on the results, observational data collected from 8 August to 10 August 2024, when meteorological conditions were similar, were averaged and used as the input for subsequent analyses.

To ensure adequate ventilation around the sensors and reduce the direct influence of solar shortwave radiation on the measurements, a TES-1365 temperature and humidity sensor and a HOBO radiation shield were mounted on the vehicle roof at approximately 1.5 m above

ISSN: 2710-0723

ground level. GPS data were recorded in real time using the *2bulu* application and matched with the microclimate data in ArcGIS based on time. Location information was recorded at 1 s intervals. Before each experiment, the sensors were calibrated, time-synchronized, and preheated to ensure data consistency. During data collection, the vehicle was driven at a stable average speed of approximately 36 km/h.

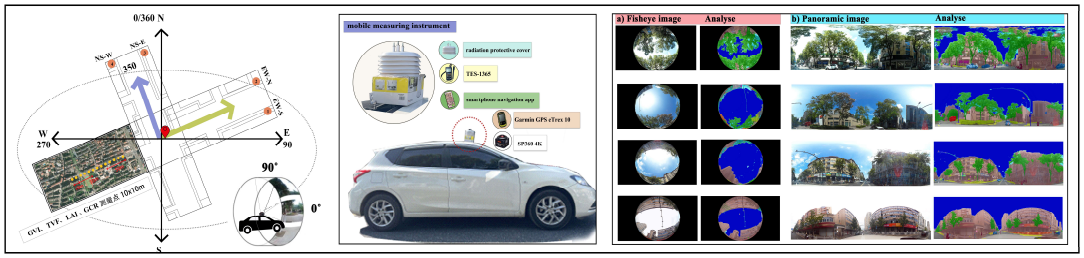

Figure 2. Street orientation, measurement instruments, photography capture points and resolution, and image processing.

2.3. Acquisition and Calculation of Street Tree Morphological Parameters

2.3.1. Acquisition of Street Tree Morphological Parameters

Tree height (TH), diameter at breast height (DBH), crown width (CW), trunk branch height (TBH), and canopy thickness (CT) were measured or estimated using a Haglöf laser rangefinder (BOSCH GLL80, accuracy = ±1.5 mm / ±0.2°). Tree canopy coverage (TCR) was calculated based on crown width and street width. Leaf area index (LAI) was measured using an LAI-2200 Plant Canopy Analyzer.

In this study, the acquisition of view-factor data was conducted simultaneously with mobile microclimate observations. A Kodak PIXPRO SP360 4K action camera was used for continuous recording. The device is equipped with a 360° spherical lens and an ultra-wide field of view of 235°. The camera was mounted on the vehicle roof, and data collection strictly complied with road traffic regulations and data privacy requirements. During data acquisition, the camera was connected via Bluetooth to the PIXPRO SP360 4K control software, enabling remote operation and real-time monitoring, and thus continuously capturing hemispherical sky images above the roadway.

The obtained VR videos were processed step by step during post-processing. First, video segments affected by traffic-related disturbances, such as stops at red lights, emergency braking, and obstacle avoidance, were removed in Adobe Premiere Pro 2025. The edited videos were then exported in SVI format as static frame images with a resolution of 2160 × 2160 pixels and a frame extraction rate of 1 frame per second. A total of 1,852 valid fisheye images of the roadway side were ultimately obtained for the calculation and analysis of GVI and TVF. Table 1 presents the street tree morphological parameters.

ISSN: 2710-0723

Table 1. Descriptive Statistics of Street Tree Characteristics

Description of Basic Characteristics	*Ginkgobiloba*	*Cinnamomum camphora*	*Zelkova schneideriana*	*Albizia julibrissin*	*Lagerstroemia indica*
Site Photographs					
Typical Fisheye Images					
Crown Shape				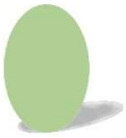	
Tree Height(m)	3-10	0-15	3-9	5-12	0-6.3
Trunk Branch Height (m)	0.9-3	0.5-4.5	0-3	2-5	0-2
Diameter at Breast Height (cm)	9-30	10-51	12-32	14-29	0-14
Crown Width (m)	2.6-7.7	0-25.3	1.75-9	3-10	0-4
Crown Volume (m^3)	36-137	0-9202	0-876	8.8-339	0-25
Canopy Thickness (m)	2-9.2	0-10	0-7	0.75-7	0-3
Tree Canopy Coverage	0-0.40	0-0.98	0-0.58	0-0.85	0-0.09
Leaf Area Index	0.30-0.45	0.19-0.78	0.29-0.38	0.27-0.39	0.07-0.15
Tree View Factor	0-0.07	0-0.64	0-0.33	0-0.54	0-0.02
Green View Index	0-0.09	0-0.45	0.01-0.21	0.01-0.39	0-0.05

2.3.2. Calculation of Street Tree Morphological Parameters

Leaf area index was calculated using HemiView software (Delta-T Devices, Cambridge, UK). Crown volume was calculated based on a geometric approximation model. Tree view factor and green view index were calculated as the proportion of the visible area identified as trees to the effective pixel area of the image. Tree canopy coverage was defined as the percentage of the total ground area covered by the summed projected canopy area of all trees. Table 3.2 presents the corresponding formulas.

ISSN: 2710-0723

Table 2. Calculation Formula

Numble	Scheme 1	Scheme 2
Crown Volume (CV)		$V=\frac{4}{3}\pi r^3$ (1) (V: volume of the sphere; π: pi; r: radius of the sphere)
		$V=\frac{4}{3}\pi r^3$ (2) (V: volume of the sphere; π: pi; r: radius of the sphere)
		$V=\frac{2}{3}\pi r^3$ (3) (V: volume of the umbrella-shaped crown; π: pi; r: radius of the sphere)
		$V=\frac{4}{3}\pi abc$ (4) (a: semi-axis length of the ellipse in the x-direction; b: semi-axis length of the ellipse in the y-direction; c: semi-axis length of the ellipsoid in the z-direction)
Leaf Area Index (LAI)	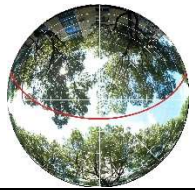	$LAI=\frac{A_{leaf}}{A_{ground}}$ (5) (LAI: leaf area index; A_leaf: total leaf area; A_ground: ground projected area (m^2))
Tree View Factor (TVF)	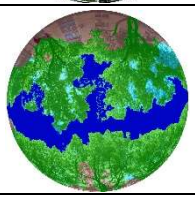	$TVF=\frac{A_{tree}}{A_{visible}}$ (6) (TVF: tree view factor; A_tree: visible area identified as trees in the image; A_visible: effective pixel area of the entire image)
Green View Index (GVI)	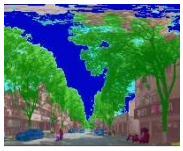	$GVI=\frac{A_{green}}{A_{visible}}$ (7) (Agreen: green visible area of trees in the image; Avisible: effective visible area)
Tree Canopy Coverage (TCR)		$TCR=\frac{A_c}{A_t}\times 100\%$ (8) (Ac: canopy coverage area, referring to the sum of the projected ground areas of all tree crowns; At: total ground area)

Do not number your paper: All manuscripts must be in English, also the table and figure texts, otherwise we cannot publish your paper. Please keep a second copy of your manuscript in your office. When receiving the paper, we assume that the corresponding authors grant us the copyright to use the paper for the book or journal in question. Should authors use tables or figures from other Publications, they must ask the corresponding publishers to grant them the right to publish this material in their paper. Use italic for emphasizing a word or phrase. Do not use boldface typing or capital letters except for section headings (cf. remarks on section headings, below).

2.4. Buffer Zone Selection

To explore the scale sensitivity of tree morphological characteristics, buffer zone analysis was necessary [222], [223]. Based on previous studies, seven buffer radii (10, 20, 50, 70, 100, 110,

ISSN: 2710-0723

and 120 m) were created around each sampling point, and the mean values of morphological parameters within these buffers were calculated in ArcGIS. Multiple linear regression analysis was then conducted to relate tree morphological indicators to directly measured microclimate data in order to determine the optimal buffer radius. This was generally consistent with the findings of Yan et al. (2018) and Hu et al. (2023) [129], [28].

2.5. Data Analysis

First, background meteorological data from the Lanling Community weather station in Lin'an District during July and August were collected. Based on these data, air temperature variation at each observation point was calculated, and the temperature values obtained from mobile measurements were standardized to two reference time points corresponding to the start of each measurement period (14:00 and 22:00), so as to improve the comparability of data among different street segments and time periods. To reduce the influence of random errors from single-day observations, four consecutive days with stable and similar meteorological conditions were further selected, and the air temperature at each sampling point was averaged to represent its thermal environment status. Under the constraint of temporal consistency, spatiotemporal relationships among air temperature, morphological indicators, and the geographic coordinates of each measurement point were established. ArcGIS was then used to generate spatiotemporal distribution maps of air temperature along the entire route and spatial distribution maps of street-tree structural and morphological characteristics, so as to characterize the spatial heterogeneity of the street-scale thermal environment and spatial form factors. The spatial verification of measurement trajectories was conducted using Google Earth imagery, and abnormal points generated in special spatial units such as road intersections were identified and removed. After data screening, 958 valid daytime samples and 859 valid nighttime samples were retained.

3. Results and Analysis

3.1. Distribution Characteristics of Street Tree Morphological Structure

Figure 3 shows the spatial distribution patterns of two-dimensional (2D) and three-dimensional (3D) greening structural and morphological indicators of street trees in the study area of Lin'an. Overall, all indicators exhibited significant spatial heterogeneity along street segments.

For the three-dimensional indicators (Fig. 3a–e), GVI ranged from 0.00 to 0.45, TVF from 0 to 0.64, LAI from 0 to 0.78, CV from 0 to 9202 m^3, and CT from 0 to 10.00 m. Both GVI and TVF ranged from 0 to 1, with smaller values indicating a lower proportion of the corresponding element in the image. In terms of spatial correspondence, streets with higher GVI generally also showed higher TVF, indicating that these street segments had more visible greenery from the pedestrian perspective.

For the two-dimensional indicators (Fig. 3f–j), TCR ranged from 0.11 to 0.98, DBH from 0 to 51 cm, TH from 0 to 15 m, CW from 0 to 25.3 m, and TBH from 0 to 5 m. TH, DBH, and CW showed similar spatial variation patterns, with their highest values mostly occurring along the same group of street segments. These segments also tended to correspond to higher tree canopy coverage (TCR), indicating more continuous canopy cover. These spatial distribution characteristics provide a basis for the subsequent quantification of the contributions of different greening structural indicators to street microclimate and their threshold effects.

ISSN: 2710-0723

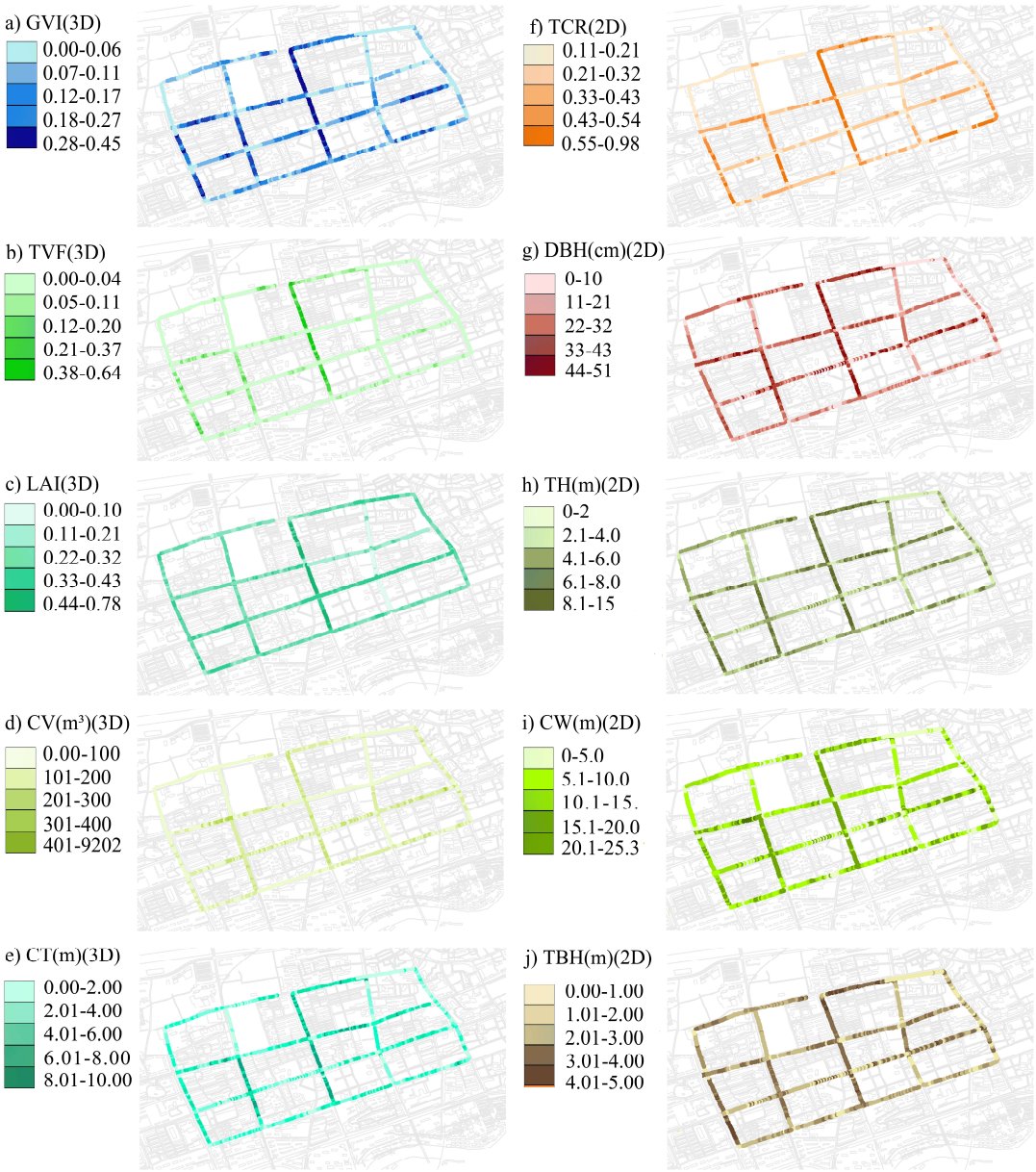

Figure 3. Street orientation, measurement instruments, photography capture points and resolution, and image processing.

3.2. Spatiotemporal Distribution Characteristics of Street Air Temperature

Figure 4 shows the spatial distribution of air temperature and its variation during the daytime (14:00–15:00). Overall, daytime air temperature reached as high as 41.9°C (Fig. 4a). In terms of spatial pattern, high temperatures were mainly concentrated on street segments with sparse vegetation and east–west (E–W) orientation, such as Chengzhong Street and Qianwang Street. Among all street canyons, areas without street trees exhibited higher temperatures than those with street trees during both daytime and nighttime. In contrast, sidewalks, which are usually located on both sides of the roadway, were more strongly influenced by shading from adjacent buildings and street tree canopies, and therefore generally showed lower air temperatures.

Notably, the temperature difference between the two sides of the same street was closely related to their spatial structural characteristics. The lowest temperature was recorded at Site S1 on Jinjiang Road, whereas the largest temperature difference, reaching 2.72°C, was observed at Site S2 on Chengzhong Street. At Site S1, the street-tree greening characteristics were GVI =

ISSN: 2710-0723

0.38, TVF = 0.64, LAI = 0.78, CV = 9202 m^3, CT = 10, TCR = 0.98, DBH = 51, TH = 15, CW = 25, and TBH = 4, indicating strong canopy enclosure and shading capacity, which could effectively block solar radiation. In contrast, at Site S2 on Chengzhong Street, GVI = 0.09, TVF = 0.07, LAI = 0.30, CV = 137 m^3, CT = 5, TCR = 0.30, DBH = 30, TH = 8, CW = 6, and TBH = 4, indicating limited canopy enclosure and a greater tendency for radiative heating and heat accumulation (Fig. 4c). Overall, streets with higher structural and morphological index values warmed more slowly. These results indicate that street-tree morphological and structural characteristics play an important role in regulating the daytime street thermal environment.

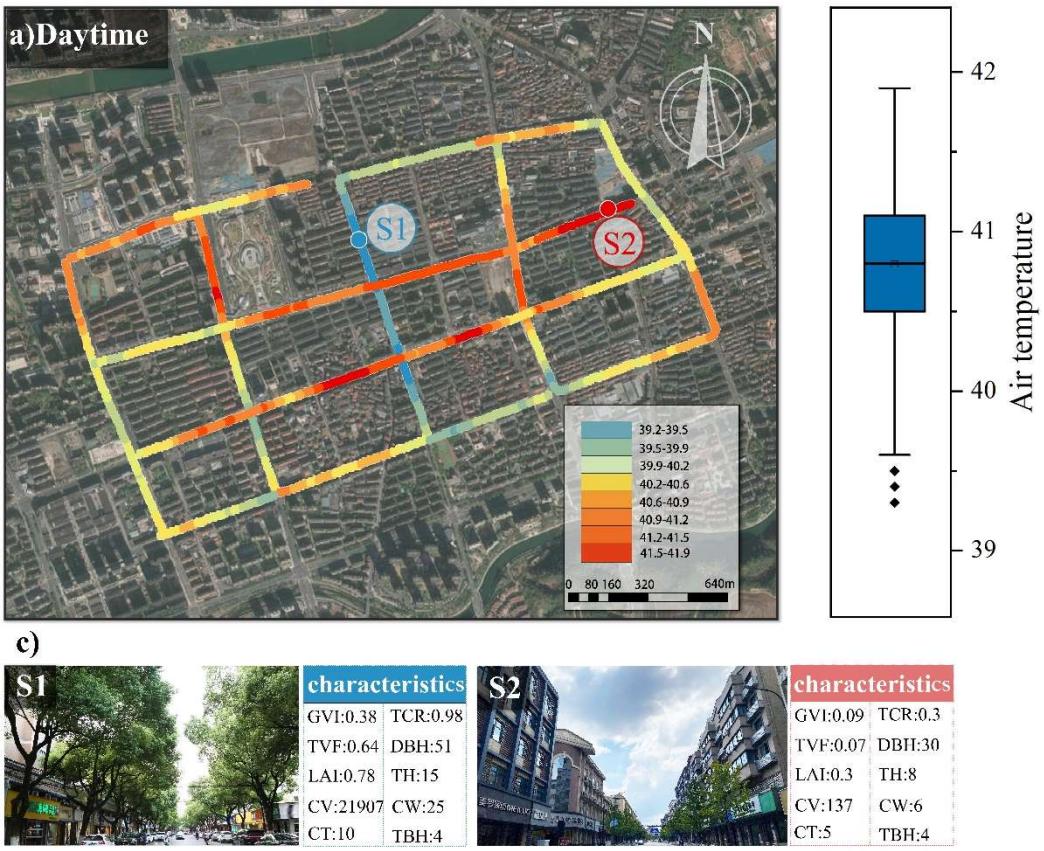

Figure 4. Street orientation, measurement instruments, photography capture points and resolution, and image processing.

Figure 5 presents the spatial distribution of air temperature and its variation at night (22:00–23:00). Compared with the daytime, nighttime air temperature decreased significantly overall, ranging from 30 to 32.40°C, while spatial differences became more pronounced (Fig. 5b). The largest nighttime temperature difference occurred between Site S3 on Xinmin Street and Site S4 on Jinjiang Road (located on the same street as S1). At Site S3, the air temperature was 30°C, which was 2.65°C higher than that at S4. At this site, GVI was only 0.02, while TVF and TCR were both 0.01, LAI was 0.2, CV was 23 m^3, CT was 3, DBH was 16, TH was 6, CW was 4, and TBH was 2 (Fig. 5c). The nighttime thermal environment at this street was more stable, which may be related to its lower TCR and TVF. Greater sky openness is more conducive to upward heat transfer and longwave radiative dissipation, thereby accelerating surface cooling. The coldest point during the daytime (S1) and the hottest point at night (S4) were located on the same street, indicating that although higher TCR and TVF can reduce radiation through shading during the daytime, they may also inhibit longwave radiative release from the surface to the sky and the upward transport of heat flux at night, resulting in near-surface heat retention and

ISSN: 2710-0723

a slower cooling process. Overall, higher GVI, TVF, and TCR can mitigate heat during the daytime, but due to stronger spatial enclosure, they are more likely to cause heat retention in the evening and at night, thereby reducing the nighttime cooling rate.

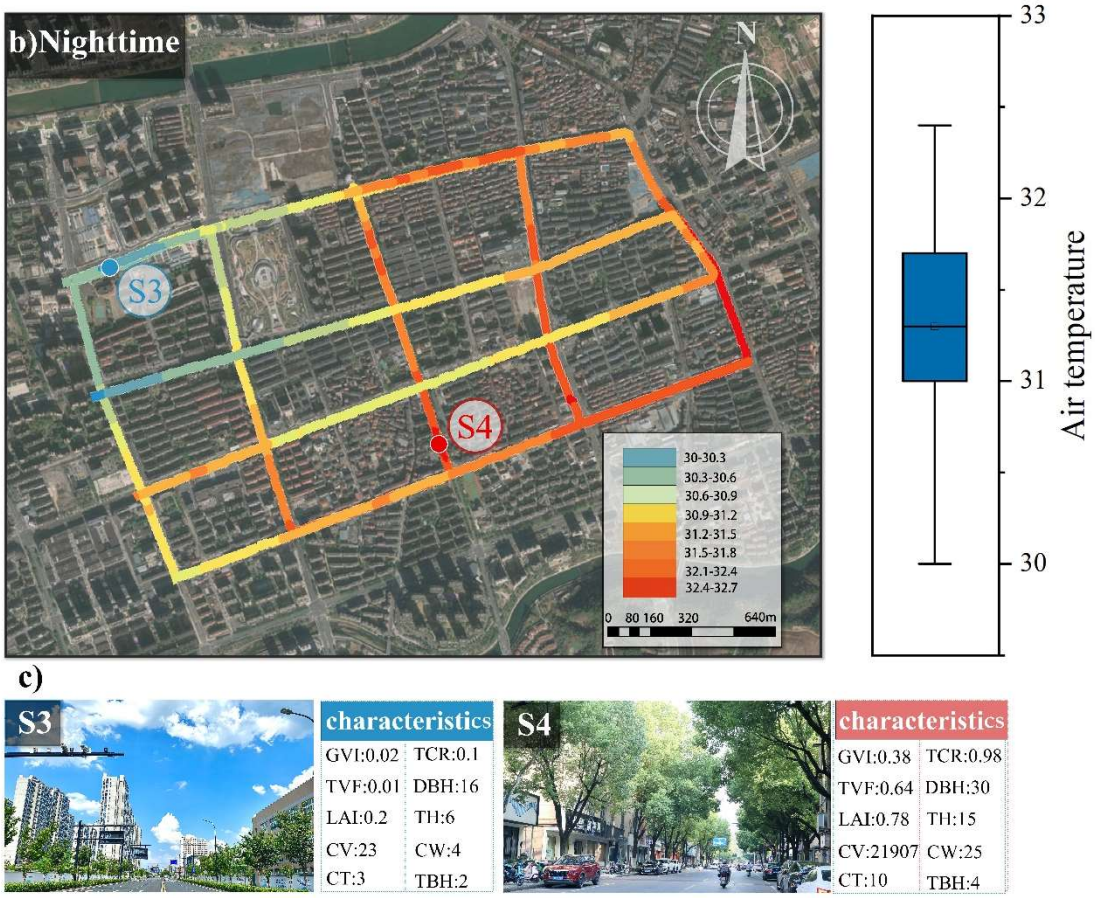

Figure 5. Spatiotemporal distribution of nighttime street air temperature.

3.3. Scale Effect

Figure 6 shows the variation in the regression performance (Adjusted R^2) of multiple street-tree morphological and structural characteristics on daytime and nighttime air temperature across different buffer scales. Within the tested buffer radii of ≤120 m, the regression results indicated significant differences in model fit across spatial scales (Fig. 6). For overall air temperature (Ta), the Adjusted R^2 values for both daytime and nighttime increased with buffer radius and peaked within the 70–110 m range. Specifically, nighttime air temperature showed the highest Adjusted R^2 at 100 m (approximately 0.09), whereas the best model fit for daytime air temperature and heat index occurred within the 100–110 m buffer range (approximately 0.55 and 0.33, respectively).

In the factor-specific analysis (Fig. 6), under daytime conditions, TCR, TVF, and GVI showed relatively high explanatory power, all of which increased steadily with buffer radius, with TVF showing the strongest explanatory ability. Under nighttime conditions, TCR explained air temperature substantially better than the other factors and reached its peak at 100 m (Adjusted $R^2 \approx 0.085$). In contrast, the other factors generally showed lower explanatory power and tended to decline after 100 m.

ISSN: 2710-0723

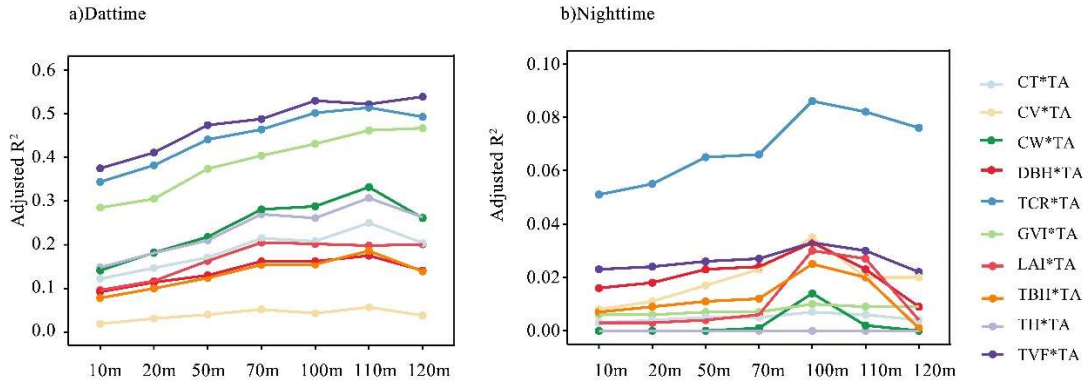

Figure 6. Regression performance (adjusted R^2) of multiple greening features for daytime and nighttime air temperature across different buffer sizes.

3.4. Correlation Analysis between Street-Tree Greening Morphological and Structural Indicators and the Thermal Environment

Figure 7 presents the correlation analysis between thermal environment indicators and street-tree greening morphological and structural characteristics during summer midday and nighttime periods. The results showed that during the daytime, except for leaf area index (LAI), all indicators were negatively correlated with air temperature and positively correlated with relative humidity. Among them, tree view factor (TVF), tree canopy coverage (TCR), green view index (GVI), crown volume (CV), crown width (CW), and tree height (TH) were all significantly negatively correlated with air temperature (Ta) ($p < 0.001$). Crown volume (CV) and green view index (GVI) were significantly negatively correlated with relative humidity (RH) ($p < 0.001$). These results indicate that TVF, TCR, CW, CV, TH, and GVI are important factors affecting under-canopy microclimate regulation.

At night, the correlations between these indicators and the microclimate were substantially weaker. Tree canopy coverage (TCR) showed a significant positive correlation with air temperature (Ta) ($p < 0.001$), whereas diameter at breast height (DBH), green view index (GVI), tree height (TH), and trunk branch height (TBH) were negatively correlated with air temperature (Ta). This indicates that the influence of street trees at night was relatively weak. Among the indicators, TCR had a warming effect on nighttime air temperature, whereas GVI, DBH, and TH had slight cooling effects.

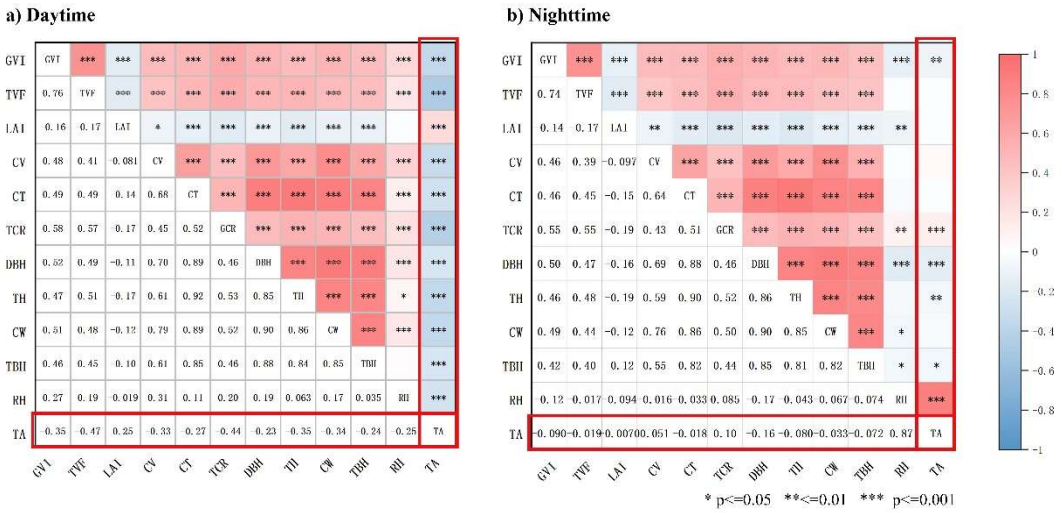

Figure 7. Correlation analysis between the street thermal environment and the morphological-structural characteristics of street trees.

ISSN: 2710-0723

Figure 8a shows the relative contribution weights of two-dimensional and three-dimensional street-tree greening morphological and structural indicators to variations in daytime thermal environment parameters. Among them, three-dimensional (3D) street-tree greening morphological and structural indicators were the primary contributors to the daytime thermal regulation effect of street trees, with an average contribution rate of 54.4%. Figures 8b and 8c further present the weight proportions of each indicator in relation to variations in different thermal environment parameters. Overall, green view index (GVI), tree view factor (TVF), and crown volume (CV) consistently played key roles in the improvement of the thermal environment by street trees, with average contributions of 14%, 13.3%, and 15%, respectively. In contrast, the contribution of two-dimensional indicators was relatively moderate, with an average contribution rate of 45.61%. Although the overall influence of two-dimensional indicators was smaller, tree canopy coverage (TCR) and crown width (CW) each contributed more than 10%, indicating that greater canopy cover may also play an important role in reducing heat exposure and improving pedestrian thermal conditions.

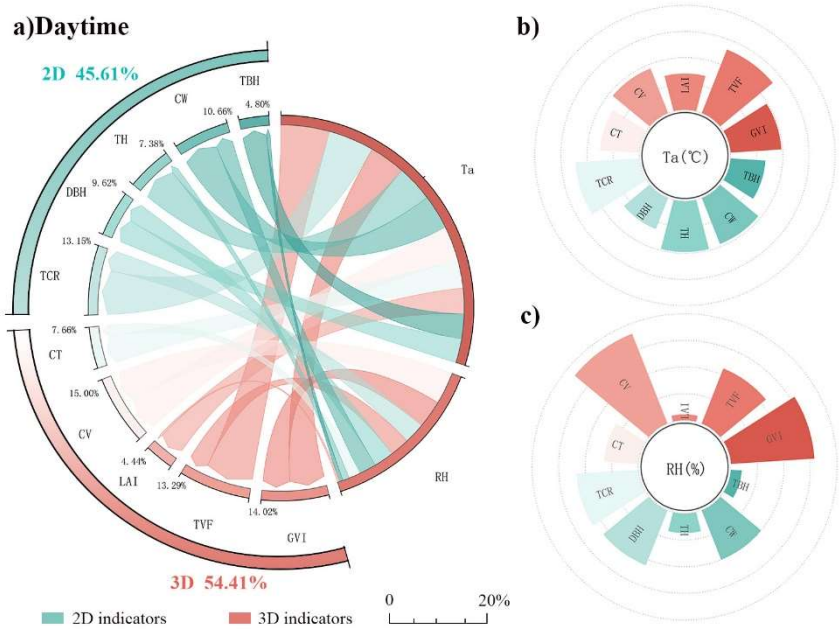

Figure 8. Contribution analysis of street-tree green structural and morphological indicators to daytime microclimate improvement.

Figure 9d shows the relative contribution weights of two-dimensional and three-dimensional street-tree greening morphological and structural indicators to variations in nighttime thermal environment parameters. Among them, two-dimensional (2D) street-tree greening morphological and structural indicators were the primary contributors to the nighttime thermal regulation effect of street trees, with an average contribution rate of 65.8%. Figures 8e and 8f further describe the weight proportions of each indicator in relation to variations in different thermal environment parameters. Overall, in the improvement of the nighttime thermal environment by street trees, green view index (GVI), tree view factor (TVF), and diameter at breast height (DBH) consistently played key roles, with average contributions of 15.5%, 13.8%, and 24.5%, respectively. In contrast, the contribution of three-dimensional indicators was relatively moderate, with an average contribution rate of 34.1%.

ISSN: 2710-0723

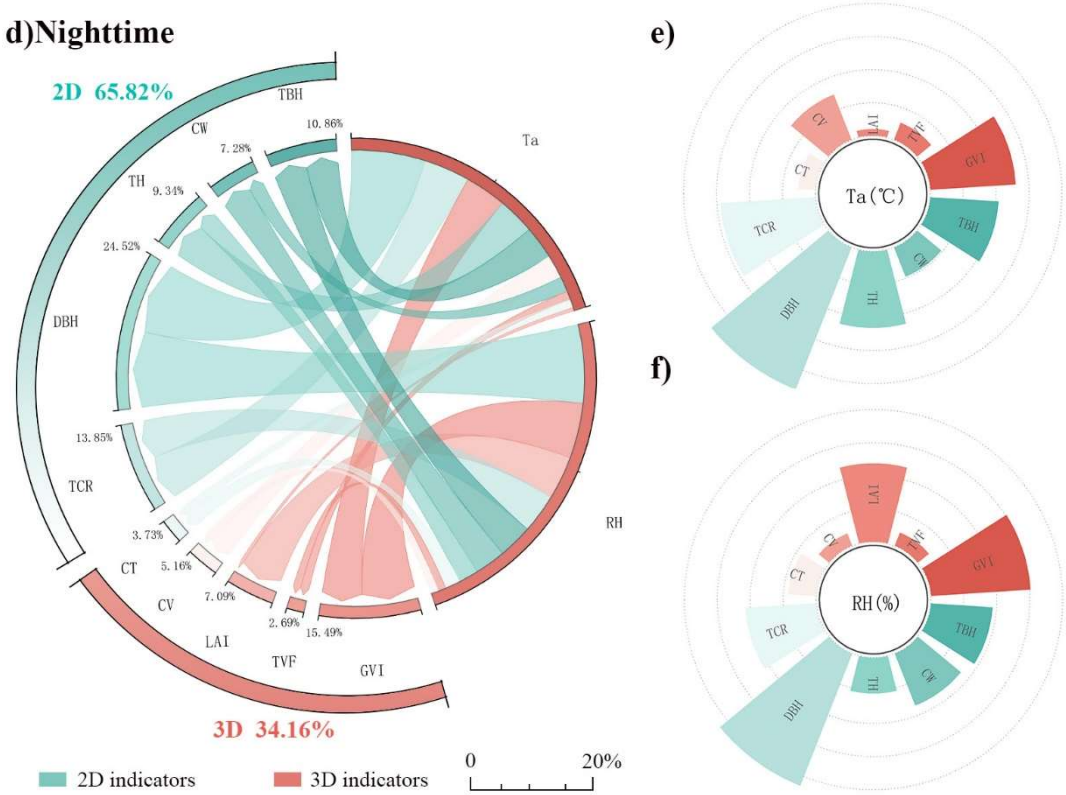

Figure 9. Contribution analysis of street-tree greening morphological–structural indicators to nighttime microclimate improvement

4. Discussion

4.1. Differences in the Street Thermal Environment

The results of this study show that the two-dimensional and three-dimensional greening morphological and structural characteristics of street trees differed markedly among streets within the study area. Combined with the spatiotemporal distribution of the street thermal environment, it can be seen that daytime air temperature reached as high as 41.9°C, and high-temperature streets were mainly associated with lower GVI, TVF, TCR, and CV, whereas streets with higher three-dimensional greening structural indicators of street trees tended to have relatively lower air temperatures [36]–[38]. This indicates that under strong daytime radiation, the greening morphological and structural characteristics of street trees reduce shortwave radiation input through canopy shading, thereby lowering the heating intensity of the ground surface and near-ground air. At the same time, tree transpiration can promote the conversion of sensible heat into latent heat, further suppressing the rise in air temperature. Previous studies have shown that the daytime cooling effect of street trees mainly results from shading and transpiration, and that greener spaces with more continuous canopies and larger canopy volumes usually exhibit stronger daytime cooling capacity [22], [39]–[41]. The findings of this study further support this conclusion.

Unlike daytime conditions, although nighttime air temperature decreased overall, its spatial distribution remained highly heterogeneous. Notably, the coldest point during the day and the relatively warm point at night were located on the same street. This suggests that streets with high TCR, high TVF, and high GVI, which exhibit a clear cooling effect during the daytime, may instead show warming effects at night. The reason is that although higher greening structural indicators can effectively block solar radiation during the day, they may also reduce longwave radiative heat dissipation from the street canyon to the sky at night and weaken upward heat

ISSN: 2710-0723

transport and air exchange near the ground, thereby slowing the cooling process. In other words, the effects of street-tree greening morphological and structural characteristics on the street thermal environment are not entirely consistent between day and night: daytime conditions are dominated by cooling effects, whereas nighttime conditions may exhibit a certain degree of heat retention [9], [42]. In addition, streets without street trees showed higher Ta during both daytime and nighttime, reflecting the significant role of street trees in reducing the thermal load of street canyons [43]. Identifying thermal differences among streets is of great significance for locating heat-retention zones and formulating targeted cooling strategies.

4.2. Differences in the Street Thermal Environment

This study found that both two-dimensional and three-dimensional greening indicators exert cooling effects on the street thermal environment, but the contribution of three-dimensional indicators to thermal improvement was more prominent, reaching 54.4%. This process is mainly achieved through higher GVI (14%), TVF (13.3%), and CV (15%), which enhance canopy enclosure and volumetric advantages from a three-dimensional spatial structural perspective. The mechanisms can be explained as follows. On the one hand, higher GVI [44]–[46], TVF [8], [47], [48], and CV enhance shading from a three-dimensional perspective, thereby providing stronger interception of incoming shortwave solar radiation above the street canyon and reducing radiative heating of road surfaces, building interfaces, and near-ground air. On the other hand, larger canopy volume usually implies greater leaf area and stronger transpiration potential, which can further reduce heat accumulation through evapotranspiration. This is consistent with the view proposed by Rahman et al. that canopy volume is an important structural variable for explaining variations in under-canopy air temperature [14], [49].

In contrast, the nighttime pattern was reversed. The overall correlations between these indicators and the thermal environment weakened, among which TCR showed a positive correlation with Ta, whereas GVI and some morphological indicators still exhibited slight cooling effects. The contribution rate of two-dimensional indicators reached 65.8%, which was significantly higher than that of three-dimensional indicators, with DBH showing the highest contribution. This may be because DBH can, to some extent, represent the health condition and overall structural size of street trees [50].

Overall, daytime cooling mainly relies on three-dimensional structures that provide shading and transpiration cooling, whereas nighttime conditions are more strongly influenced by two-dimensional coverage characteristics, which may hinder longwave radiation from the street toward the sky. Therefore, optimization of the street thermal environment should not focus solely on increasing tree canopy coverage, but should place greater emphasis on the three-dimensional indicators of street-tree greening morphological and structural characteristics.

4.3. Effects of Scale on the Street Thermal Environmen

The effects of street-tree greening morphological and structural characteristics on street air temperature showed a certain degree of spatial scale dependence. Overall, the performance of both daytime and nighttime models increased with buffer radius and reached relatively high levels within the range of 70–110 m, with the best daytime fit concentrated within 100–110 m and the nighttime peak occurring at around 100 m. These results indicate that the regulating effects of street trees on the street thermal environment do not occur only at the scale of individual trees or single points, but rather manifest as an integrated effect over a certain street-segment range. This finding is generally consistent with previous studies showing that the cooling effect of urban trees has a distinct spatial extent and buffer range, and is also in agreement with the LCZ framework, which emphasizes that thermal environment analysis should match the corresponding spatial unit [1], [6], [35], [51], [52].

ISSN: 2710-0723

More specifically, the explanatory power of TCR, TVF, and GVI increased gradually with scale under daytime conditions, indicating that daytime street temperature is influenced not only by local canopy shading but also by the accumulation of three-dimensional greenery. In other words, daytime cooling is more of an overall street-segment-scale effect rather than the isolated effect of individual trees. By contrast, except for TCR, the explanatory power of the remaining indicators was generally weak at night and declined after 100 m, suggesting that the influence range of street-tree greening morphological and structural characteristics is relatively limited at night and more easily affected by the background thermal environment and local heat dissipation conditions. Previous studies have shown that the cooling effect of greenery is not instantaneous or point-based, but generally depends on the organization of greenery and heat exchange processes within a certain spatial range; at the same time, the cooling effect of street trees usually gradually decays with distance [53].

4.4. Limitations

This study used field observations to capture the characteristics of the street thermal environment with relatively high accuracy. However, several limitations remain.

First, the study area is located in Lin'an District, Hangzhou, a city with a subtropical monsoon climate. Although the area has relatively abundant street-tree resources and is somewhat representative, the generalizability of the findings to other climate zones and different urban forms remains limited. Future studies should include cities in arid, temperate, and tropical climates to improve the external validity of the results.

Second, field measurements were conducted in a complex urban environment, where spatial heterogeneity in street canyon morphology, wind environment, and land-cover type is difficult to avoid.

Finally, this study focused only on air temperature and did not simultaneously measure other key microclimatic factors such as relative humidity, wind speed, and solar radiation. Therefore, a more comprehensive assessment of thermal comfort could not yet be carried out. Given that pedestrian thermal perception is jointly affected by multiple environmental factors, future work should incorporate more microclimatic parameters and combine them with thermal comfort indices such as mean radiant temperature (MRT) or physiological equivalent temperature (PET) to characterize pedestrian-scale thermal experience more accurately. Accordingly, subsequent studies should be extended to more climate zones and should combine MRT, PET, and similar indicators to conduct more comprehensive pedestrian-scale thermal environment analyses, thereby further verifying the mechanisms through which street-tree greening morphological and structural characteristics affect the street thermal environment.

5. Conclusion

If you follow the "checklist" your paper will conform to the requirements of the publisher and facilitate a problem-free publication process.

This study focused on Lin'an District, Hangzhou, a city in China with a subtropical monsoon climate, and analyzed the effects of street-tree greening morphological and structural characteristics on the street thermal environment based on a mobile measurement system. From the perspectives of two-dimensional and three-dimensional structures, the study revealed the daytime and nighttime differences in the street thermal environment under different street-tree greening morphological and structural characteristics, compared the relative contributions of two-dimensional and three-dimensional indicators to air temperature, and identified the key structural factors affecting the street thermal environment. The main conclusions are as follows:

ISSN: 2710-0723

(1) Different street-tree greening morphological and structural characteristics exert different effects on the street thermal environment, with clear daytime–nighttime differences. The results show that the two-dimensional and three-dimensional greening morphological and structural indicators of street trees in the study area exhibited obvious spatial heterogeneity along street segments, and street air temperature also showed significant spatiotemporal variation. High-temperature street segments during the daytime were mainly associated with lower GVI, TVF, TCR, and CV, whereas street segments with higher greening structural indicators had relatively lower air temperatures, indicating that stronger canopy enclosure and larger canopy volume help slow the warming process. Although nighttime air temperature was significantly lower overall than daytime temperature, spatial differences remained pronounced, and street segments with significant daytime cooling effects did not necessarily maintain a cooling advantage at night. This indicates that the regulating effects of street-tree greening morphological and structural characteristics on the street thermal environment are not entirely consistent between day and night: daytime conditions are dominated by cooling through shading and transpiration, whereas nighttime conditions may experience slower heat dissipation due to enhanced spatial enclosure. Meanwhile, streets without street trees exhibited higher air temperatures during both day and night, further demonstrating the important role of street trees in reducing street thermal load.

(2) Both two-dimensional and three-dimensional street-tree greening morphological and structural indicators have cooling effects, but three-dimensional indicators are more dominant during the daytime, whereas two-dimensional indicators play a more prominent role at night. Under daytime conditions, the average contribution rate of three-dimensional greening morphological and structural indicators to improving the street thermal environment reached 54.4%, which was higher than the 45.61% contributed by two-dimensional indicators. Among them, GVI, TVF, and CV were the most critical structural factors during the daytime, with average contributions of 14%, 13.3%, and 15%, respectively, indicating that pedestrian-perspective greenery, overhead canopy enclosure, and canopy volumetric advantages form the key structural basis for daytime street cooling. At night, however, the opposite trend was observed: the average contribution rate of two-dimensional indicators reached 65.8%, significantly higher than the 34.1% contributed by three-dimensional indicators, among which DBH showed the highest contribution, while GVI and TVF still maintained some influence. Overall, daytime street cooling mainly depends on the shading and transpiration cooling effects provided by three-dimensional structures, whereas nighttime conditions are more affected by two-dimensional coverage characteristics and the physical structure of trees. This suggests that the regulatory mechanism of street trees on the street thermal environment cannot be fully explained solely from planar canopy coverage or single-tree-scale indicators, and instead requires a comprehensive analysis from the coordinated perspectives of both two-dimensional and three-dimensional structures.

(3) GVI, TVF, TCR, CV, TH, CW, and DBH are the key structural factors affecting street air temperature, but their cooling performance differs significantly between daytime and nighttime and shows a certain degree of spatial scale dependence. Correlation analysis showed that, except for LAI, most greening morphological and structural indicators were negatively correlated with air temperature during the daytime. Among them, TVF, TCR, GVI, CV, CW, and TH were most significantly related to Ta, indicating that these indicators are important factors affecting under-canopy microclimate regulation. At night, the correlations between these indicators and the thermal environment weakened overall. Among them, TCR was positively correlated with Ta, whereas GVI, DBH, TH, and TBH still showed certain cooling effects, indicating that nighttime thermal regulation is more closely related to canopy continuity, tree size, and spatial openness. Buffer analysis further showed that the influence of street-tree greening morphological and structural characteristics on air temperature has a clear spatial

ISSN: 2710-0723

scale dependence, with approximately 70–110 m being the optimal range, among which the best daytime fit was concentrated within 100–110 m, while nighttime conditions peaked at around 100 m. This indicates that the cooling performance of key structural factors does not occur only at the scale of individual trees or single points, but rather manifests as a spatially accumulated effect over a certain street-segment range.

In summary, the regulation of the street thermal environment by street trees is closely related to their greening morphological and structural characteristics. Future optimization of street greening should shift from simply increasing canopy coverage to the coordinated configuration of two-dimensional and three-dimensional structures. For street segments with severe daytime heat exposure, priority should be given to increasing GVI, TVF, and CV to enhance canopy enclosure and transpiration cooling capacity. For street segments with a higher risk of nighttime heat retention, excessively high TCR and canopy continuity should be appropriately controlled to balance daytime cooling and nighttime heat dissipation. At the same time, optimization of the street thermal environment should not remain at the level of individual-tree configuration, but should instead take street segments of around 100 m as the basic organizational unit and comprehensively consider the coordinated effects of street-tree structural characteristics. From the perspectives of two-dimensional and three-dimensional structures, this study reveals the differentiated regulatory patterns of street-tree greening morphological and structural characteristics on street air temperature and provides empirical evidence for street-greening optimization and climate-adaptive urban thermal environment design.

References

[1] I.D. Stewart and T.R. Oke: Local climate zones for urban temperature studies, Bulletin of the American Meteorological Society, Vol. 93 (2012) No. 12, p.1879-1900.

[2] T.R. Oke: Street design and urban canopy layer climate, Energy and Buildings, Vol. 11 (1988) No. 1, p.103-113.

[3] J. Ballester et al.: Heat-related mortality in Europe during the summer of 2022, Nature Medicine, Vol. 29 (2023) No. 7, p.1857-1866.

[4] K.L. Ebi et al.: Hot weather and heat extremes: health risks, The Lancet, Vol. 398 (2021) No. 10301, p.698-708.

[5] F. Ali-Toudert and H. Mayer: Numerical study on the effects of aspect ratio and orientation of an urban street canyon on outdoor thermal comfort in hot and dry climate, Building and Environment, Vol. 41 (2006), p.94-108.

[6] Y. Hu et al.: Which street is hotter? Street morphology may hold clues-thermal environment mapping based on street view imagery, Building and Environment, Vol. 262 (2024), p.111838.

[7] C. Sun, W. Lian, L. Liu, Q. Dong and Y. Han: The impact of street geometry on outdoor thermal comfort within three different urban forms in severe cold region of China, Building and Environment, Vol. 222 (2022), p.109342.

[8] Z. Zhao et al.: Air temperature differences and view factor influences between sidewalks and roadways in urban streets: A case study in Hangzhou, China, Building and Environment, Vol. 290 (2026), p.114149.

[9] N. Meili et al.: Tree effects on urban microclimate: diurnal, seasonal, and climatic temperature differences explained by separating radiation, evapotranspiration, and roughness effects, Urban Forestry & Urban Greening, Vol. 58 (2021), p.126970.

[10] R. Sanusi, D. Johnstone, P. May and S.J. Livesley: Microclimate benefits that different street tree species provide to sidewalk pedestrians relate to differences in plant area index, Landscape and Urban Planning, Vol. 157 (2017), p.502-511.

[11] J.L. Moss, K.J. Doick, S. Smith and M. Shahrestani: Influence of evaporative cooling by urban forests on cooling demand in cities, Urban Forestry & Urban Greening, Vol. 37 (2019), p.65-73.

ISSN: 2710-0723

[12] Z. Ren, H. Zhao, Y. Fu, L. Xiao and Y. Dong: Effects of urban street trees on human thermal comfort and physiological indices: A case study in Changchun City, China, Journal of Forestry Research, Vol. 33 (2022) No. 3, p.911-922.

[13] B.M. de Quadros and M.G.O. Mizgier: Urban green infrastructures to improve pedestrian thermal comfort: A systematic review, Urban Forestry & Urban Greening, Vol. 88 (2023), p.128091.

[14] M.A. Rahman et al.: Traits of trees for cooling urban heat islands: A meta-analysis, Building and Environment, Vol. 170 (2020), p.106606.

[15] A. Coombes, J. Martin and D. Slater: Defining the allometry of stem and crown diameter of urban trees, Urban Forestry & Urban Greening, Vol. 44 (2019), p.126421.

[16] Y. Zhao, H. Li, R. Bardhan, A. Kubilay, Q. Li and J. Carmeliet: The time-evolving impact of tree size on nighttime street canyon microclimate: Wind tunnel modeling of aerodynamic effects and heat removal, Urban Climate, Vol. 49 (2023), p.101528.

[17] A. Speak, L. Montagnani, C. Wellstein and S. Zerbe: The influence of tree traits on urban ground surface shade cooling, Landscape and Urban Planning, Vol. 197 (2020), p.103748.

[18] Y. Zhao, Y. Chen and K. Li: A simulation study on the effects of tree height variations on the façade temperature of enclosed courtyard in North China, Building and Environment, Vol. 207 (2022), p.108566.

[19] W. Zhou et al.: Urban tree canopy has greater cooling effects in socially vulnerable communities in the US, One Earth, Vol. 4 (2021) No. 12, p.1764-1775.

[20] M.A. Rahman et al.: More than a canopy cover metric: influence of canopy quality, water-use strategies and site climate on urban forest cooling potential, Landscape and Urban Planning, Vol. 248 (2024), p.105089.

[21] X. Zheng et al.: Influence of vertical greenery systems with different greenery coverage ratios on microclimate improvement in street canyons by scaled outdoor experiments, Building and Environment, Vol. 267 (2025), p.112158.

[22] T.E. Morakinyo, L. Kong, K.K.-L. Lau, C. Yuan and E. Ng: A study on the impact of shadow-cast and tree species on in-canyon and neighborhood's thermal comfort, Building and Environment, Vol. 115 (2017), p.1-17.

[23] K.Y. Cheng, K. Lau, Y.T. Shek, Z. Liu and E. Ng: Evaluation on the performance of tree view factor in a high-density subtropical city: A case study in Hong Kong, Building and Environment, Vol. 239 (2023), p.110431.

[24] Y. Cai et al.: Effect of the roadside tree canopy structure and the surroundings on the daytime urban air temperature in summer, Agricultural and Forest Meteorology, Vol. 316 (2022), p.108850.

[25] H. Li, Y. Zhao, C. Wang, D. Ürge-Vorsatz, J. Carmeliet and R. Bardhan: Cooling efficacy of trees across cities is determined by background climate, urban morphology, and tree trait, Communications Earth & Environment, Vol. 5 (2024) No. 1, p.754.

[26] A. Wujeska-Klause and S. Pfautsch: The best urban trees for daytime cooling leave nights slightly warmer, Forests, Vol. 11 (2020) No. 9, p.945.

[27] T.E. Morakinyo and Y.F. Lam: Simulation study on the impact of tree-configuration, planting pattern and wind condition on street-canyon's micro-climate and thermal comfort, Building and Environment, Vol. 103 (2016), p.262-275.

[28] C.D. Ziter, E.J. Pedersen, C.J. Kucharik and M.G. Turner: Scale-dependent interactions between tree canopy cover and impervious surfaces reduce daytime urban heat during summer, Proceedings of the National Academy of Sciences, Vol. 116 (2019) No. 15, p.7575-7580.

[29] T.P. Lin, K.T. Tsai, R.L. Hwang and A. Matzarakis: Quantification of the effect of thermal indices and sky view factor on park attendance, Landscape and Urban Planning, Vol. 107 (2012) No. 2, p.137-146.

[30] C. Huang et al.: Effect of urban morphology on air pollution distribution in high-density urban blocks based on mobile monitoring and machine learning, Building and Environment, Vol. 219 (2022), p.109173.

ISSN: 2710-0723

[31] B. Zhou, S. Kaplan, A. Peeters, I. Kloog and E. Erell: "Surface," "satellite" or "simulation": Mapping intra-urban microclimate variability in a desert city, International Journal of Climatology, Vol. 40 (2020) No. 6, p.3099-3117.

[32] H. Yokoyama, R. Ooka and H. Kikumoto: Study of mobile measurements for detailed temperature distribution in a high-density urban area in Tokyo, Urban Climate, Vol. 24 (2018), p.517-528.

[33] L. Romero Rodríguez, J. Sánchez Ramos, J.L. Molina Félix and S. Álvarez Domínguez: Urban-scale air temperature estimation: development of an empirical model based on mobile transects, Sustainable Cities and Society, Vol. 63 (2020), p.102471.

[34] S. Yin, S. Xiao, X. Ding and Y. Fan: Improvement of spatial-temporal urban heat island study based on local climate zone framework: A case study of Hangzhou, China, Building and Environment, Vol. 248 (2024), p.111102.

[35] H. Yan, F. Wu and L. Dong: Influence of a large urban park on the local urban thermal environment, Science of the Total Environment, Vol. 622-623 (2018), p.882-891.

[36] T.R. Oke: Boundary Layer Climates (Routledge, UK 1987).

[37] A.J. Arnfield: Two decades of urban climate research: A review of turbulence, exchanges of energy and water, and the urban heat island, International Journal of Climatology, Vol. 23 (2003) No. 1, p.1-26.

[38] E. Erell, D. Pearlmutter and T.J. Williamson: Urban Microclimate: Designing the Spaces Between Buildings (Routledge, UK 2011).

[39] A.M. Coutts, E.C. White, N.J. Tapper, J. Beringer and S.J. Livesley: Temperature and human thermal comfort effects of street trees across three contrasting street canyon environments, Theoretical and Applied Climatology, Vol. 124 (2016) No. 1-2, p.55-68.

[40] M. Santamouris: Recent progress on urban overheating and heat island research. Integrated assessment of the energy, environmental, vulnerability and health impact. Synergies with the global climate change, Energy and Buildings, Vol. 207 (2020), p.109482.

[41] A. Aflaki et al.: Urban heat island mitigation strategies: A state-of-the-art review on Kuala Lumpur, Singapore and Hong Kong, Cities, Vol. 62 (2017), p.131-145.

[42] J. Konarska, B. Holmer, F. Lindberg and S. Thorsson: Influence of vegetation and building geometry on the spatial variations of air temperature and cooling rates in a high-latitude city, International Journal of Climatology, Vol. 36 (2016) No. 5, p.2379-2395.

[43] A.K. Ettinger et al.: Street trees provide an opportunity to mitigate urban heat and reduce risk of high heat exposure, Scientific Reports, Vol. 14 (2024) No. 1, p.3266.

[44] T.C. Chan, P.H. Lee, Y.T. Lee and J.H. Tang: Exploring the spatial association between the distribution of temperature and urban morphology with green view index, PLOS ONE, Vol. 19 (2024) No. 5, p.e0301921.

[45] Y. Lu, L. Chapman, E.J.S. Ferranti and C. Pfrang: The relationship between street greenery and daytime air temperature: A study based on parameters derived from street view images, Urban Climate, Vol. 64 (2025), p.102623.

[46] Q. Wang, Y. Hu and H. Yan: Research on the mechanism of the impact of green view index of urban streets on thermal environment: A machine learning-driven empirical study in Hangzhou, China, Atmosphere, Vol. 16 (2025) No. 5, p.617.

[47] Y. Sang et al.: Dynamic changes of urban street thermal environment from the pedestrian perspective and their impacts on pedestrians' walking behaviors, Sustainable Cities and Society, Vol. 135 (2025), p.106971.

[48] Z. Yang, B. Niu, Y. Pan and Y. Chen: Multi-objective optimization of supply air jet enhancing airflow uniformity in data center using Taguchi/CRITIC/TOPSIS triple method, Building and Environment, Vol. 244 (2023), p.110784. [Please verify relevance]

[49] L. Gratani and L. Varone: Carbon sequestration by Quercus ilex L. and Quercus pubescens Willd. and their contribution to decreasing air temperature in Rome, Urban Ecosystems, Vol. 9 (2006) No. 1, p.27-37.

ISSN: 2710-0723

[50] W. Wang et al.: Do healthier trees cool better? Assessing the impact of street tree health on urban thermal regulation and pedestrian comfort, Building and Environment, Vol. 285 (2025), p.113665.

[51] D.E. Bowler, L.M. Buyung-Ali, T.M. Knight and A.S. Pullin: Urban greening to cool towns and cities: A systematic review of the empirical evidence, Landscape and Urban Planning, Vol. 97 (2010) No. 3, p.147-155.

[52] F. Aram, E. Higueras García, E. Solgi and S. Mansournia: Urban green space cooling effect in cities, Heliyon, Vol. 5 (2019) No. 4, p.e01339.

[53] C.D. Ziter, E.J. Pedersen, C.J. Kucharik and M.G. Turner: Scale-dependent interactions between tree canopy cover and impervious surfaces reduce daytime urban heat during summer, Proceedings of the National Academy of Sciences, Vol. 116 (2019) No. 15, p.7575-7580.